Traffic Injury Prevention, 6:67–76, 2005

ISSN: 1538-9588 print / 1538-957X online
DOI: 10.1080/15389580590903203

Taylor & Francis
Taylor & Francis Group

The Effect of Muscle Activation on Neck Response

KARIN BROLIN and PETER HALLDIN
Division of Neuronic Engineering, The Royal Institute of Technology, Stockholm, Sweden

INGRID LEIJONHUFVUD
Alfgam Optimering AB, Tyresö, Sweden

Prevention of neck injuries due to complex loading, such as occurs in traffic accidents, requires knowledge of neck injury mechanisms and tolerances. The influence of muscle activation on outcome of the injuries is not clearly understood. Numerical simulations of neck injury accidents can contribute to increase the understanding of injury tolerances. The finite element (FE) method is suitable because it gives data on stress and strain of individual tissues that can be used to predict injuries based on tissue level criteria.

The aim of this study was to improve and validate an anatomically detailed FE model of the human cervical spine by implement neck musculature with passive and active material properties. Further, the effect of activation time and force on the stresses and strains in the cervical tissues were studied for dynamic loading due to frontal and lateral impacts.

The FE model used includes the seven cervical vertebrae, the spinal ligaments, the facet joints with cartilage, the intervertebral disc, the skull base connected to a rigid head, and a spring element representation of the neck musculature. The passive muscle properties were defined with bilinear force-deformation curves and the active properties were defined using a material model based on the Hill equation. The FE model's responses were compared to volunteer experiments for frontal and lateral impacts of 15 and 7 g. Then, the active muscle properties where varied to study their effect on the motion of the skull, the stress level of the cortical and trabecular bone, and the strain of the ligaments.

The FE model had a good correlation to the experimental motion corridors when the muscles activation was implemented. For the frontal impact a suitable peak muscle force was 40 N/cm^2 whereas 20 N/cm^2 was appropriate for the side impact. The stress levels in the cortical and trabecular bone were influenced by the point forces introduced by the muscle spring elements; therefore a more detailed model of muscle insertion would be preferable. The deformation of each spinal ligament was normalized with an appropriate failure deformation to predict soft tissue injury. For the frontal impact, the muscle activation turned out to mainly protect the upper cervical spine ligaments, while the musculature shielded all the ligaments disregarding spinal level for lateral impacts. It is concluded that the neck musculature does not have the same protective properties during different impacts loadings.

The neck is vulnerable to injury especially in traffic, sport, and fall accidents. A statistical survey of hospital data revealed that neck injuries from transportation accidents are dominated by the younger population while the elderly population is involved in most fall accident related neck injuries (Brolin & von Holst, 2002; Brolin, 2003). It is important to focus on preventive efforts both in the transportation and fall accident areas. Unfortunately, the lack of neck injury criteria for soft tissue injuries as well as for vertebral fractures slows the progress of neck injury prevention. It is possible to increase the understanding of the cervical spine complex, define injury criteria, and answer some of the questions using numerical analyses. The finite element (FE) method enables simulations of neck kinematics during impact with simultaneous information on the stress levels in the individual cervical tissues. This information can be compared to failure data for the specific tissues and used to predict injuries. It is possible to evaluate how the direction of impact and the boundary conditions influence the outcome of an accident. Another important factor is believed to be the neck muscle response. How and if the neck muscles are activated may change the injury mechanism or severity. There are a few numerical models that have implemented the neck muscles. Models by de Jager et al. (1994), Yang et al. (1998), and Jost and Nurick (2000) have implemented the passive properties of the muscles in their models. De Jager et al. (1996) then improved their model to include the active properties and compared it with volunteer sled data for frontal and lateral impacts. They modeled the soft tissues and rigid vertebrae. The muscles were simplified with spring elements that could not follow the neck curvature, which will lead to inaccurate lines of action for large neck motions. This was later improved by van der Horst (2002), who enabled

Received 11 November 2003; accepted 2 July 2004.
Address correspondence to Karin Brolin, Division of Neuronic Engineering, Royal Institute of Technology, Stockholm S-100 44, Sweden. E-mail: karinbr@kth.se

the muscle to curve around the vertebrae by including sliding points attached to intermediate vertebrae. Van Ee et al. (2000) developed a lumped parameter model including active and passive muscles to study tensile loading.

A detailed FE model of the cervical spine with passive muscle properties, called the KTH model, has been developed by Brolin (2002) and Halldin (2001). The KTH model was first validated at the spinal segment level, then for the complete ligamentous cervical spine, and lastly, validations were performed for the cervical spine with passive muscle properties implemented. The performed validations are:

- Compression, shear, and torsion of a motion segment in the lower cervical spine were compared to experiments by Liu et al. (1980) and Halldin (1998), presented by Halldin et al. (2000). The load-deflection responses showed good correlation and injury prediction of disc herniation was realistic.
- Flexion, extension, lateral bending, axial rotation, and tension in the upper cervical spine compared well to cadaver data by Panjabi et al. (1991a, b), Goel et al. (1990) and Van Ee et al. (2000). This study, presented by Brolin and Halldin (2003), concluded that the material properties of the ligaments are more important for the validation of joint motions than the material properties of the hard tissues. Only nondestructive loading was used and the KTH model did not predict failure based on tissues deformations and stresses.
- Compression, flexion, lateral bending, and oblique impacts of the complete ligamentous cervical spine were compared to experimental data by Nightingale et al. (1996, 1997) and Ewing et al. (1976a, b), presented by Halldin et al. (2000), Halldin (2001), and Brolin (2002). Buckling of the spine and motion for compression showed very good correlation and the boundary forces compared well with the experimental data, Halldin et al. (2000). Neck motion and accelerations were compared for the flexion, lateral and oblique impacts with good correlation in Halldin (2001) and Brolin (2002). Injury prediction based on tissue level criteria for vertebral stress data correlated with epidemiological studies of accidents with compression loading and the cadaver experiments by Nightingale et al. (1996, 1997) and Halldin et al. (2000). The simulation of Ewing's volunteer experiments (1976a, b) did not predict vertebral injuries based on tissue level criteria, as expected.
- Frontal, lateral, and oblique impacts of the complete FE model with passive muscle properties were compared to volunteer experiments by Ewing et al. (1976a, b). Data for load-deflection and accelerations of the skull relative to the torso were presented by Leijonhufvud (2001) and shows good correlation but differs at a later stage during the impact due to the lack of the KTH model to simulate the activation of the volunteer's neck musculature in response to the impact.

Van Ee et al. (2000) showed that the tensile injury tolerance of the cervical spine increased with muscle activation and that the injury location moved from the lower to the upper cervical spine. To the best of our knowledge, there are no published results of how the neck muscle activation influences the spinal injury tolerances based on tissue level criteria.

Therefore, it is the aim of this study to improve and validate an FE model of the cervical spine (the KTH model) with neck muscles that can curve around the vertebrae and implements active muscle properties. Further, the effect of the timing of the activation and the activation force on the stresses and strains in the cervical tissues will be studied for dynamic loading in frontal and lateral impacts.

METHOD

In this study, the KTH FE model of the human cervical spine was used, Figure 1. The KTH model has been developed by the authors Brolin (2002) and Halldin (2001). The FE software used was LS-DYNA, Hallquist (1998). Shortly, the KTH model includes the seven cervical vertebrae (C1-C7), the skull base, a rigid head developed by Kleiven (2002), the intervertebral discs, the facet joints with cartilage, the cervical ligaments, and the neck musculature. The first thoracic vertebra (T1) is represented by a cube, place inferior of C7. The vertebral geometry is based on computer tomography scans of a 27-year-old man and scaled to represent a 50th percentile man. Data regarding size and insertion points for the ligaments, the disc, and the neck musculature are taken from the literature, as described by Brolin and Halldin (2003), Brolin (2002), Halldin et al. (2000), Halldin (2001), and Leijonhufvud (2001). The nodes of the muscle elements were chosen according to anatomy literature by Goel et al. (1986) and Kapandji (1974). All the vertebral joints with articulate surfaces are modeled with sliding only contact definitions. Table I gives an overview of the element types and material models implemented for the different cervical tissues.

The following muscles were modeled: the sternocleidomastoid (SCM), the longus cervicis, the rectus capitis anterior major (RAMa), the rectus capitis anterior minor (RAMi), the scalenus anterior, the scalene medius and the scalene posterior (Scalene), the rectus capitis posterior major, the rectus capitis posterior minor, the inferior oblique, and the superior oblique (Suboccipital), the semispinals muscles, the longissimus capitis, the splenius capitis and splenius cervicis (Splenius), the levator scapulae, the trapezius, the interspinous muscles, the sternothyroid and thyrohyoid (Hyoid superior), and the omohyoid and strenohyoid (Hyoid inferior).

Each muscle was modeled with a number of parallel spring elements, Table II. Thereby, the muscle force is directed in a

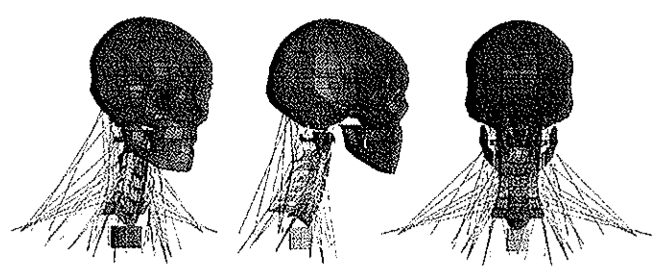

Figure 1 Three views of the human neck FE model with a rigid head and the developed neck muscles. The inferior cube represents the thorax.

Table I Material and element types implemented in the human neck FE model

Cervical tissue	Element type	Material type	Stiffness	Model I	Model II
Cortical bone	4-node shell	Linear visco-elastic	15 GPa	C1,3,5	C2,4,6
		Rigid body		C0,2,4,6,7	C0,1,3,5,7
Trabecular bone	8-node solid	Linear visco-elastic	0.5 GPa	C1,3,5	C2,4,6
		Rigid body		C0,2,4,6,7	C0,1,3,5,7
Spinal ligaments	2-node spring	Non-linear tension-only	Brolin and Halldin (2003)		
Transverse ligament	4-node membrane	Linear elastic	135/6 MPa*		
Intervertebral disc:					
AF	4-node membrane	Linear elastic, anisotropic	30/6 MPa*		
AM	8-node solid	Linear visco-elastic	3 MPa		
NP	8-node solid	Linear elastic, incompressible	1 MPa		
Cartilage	8-node solid	Linear elastic	10 MPa		
Neck musculature	2-node spring	Passive properties with damping		Table 2	
		Active properties: Hill muscle model		Table 2	

The two models I and II have different combinations of rigid and elastic elements for the bony tissues. C0: the skull base, C1–7: first to seventh cervical vertebrae.
*Stiffness in lateral/perpendicular direction. For references please see Brolin and Halldin (2003) and Halldin et al. (2000).
AF: Annulus fibrosis, AM: Annulus matrix material, NP: Nucleus pulposus.

straight line between the origin and insertion of the muscle. To account for the neck curvature the superficial neck muscles that elongate over the complete cervical spine were divided into four spring elements in series, Table II. The nodes connecting two serial spring elements were constrained to the closest rigid vertebra to force the muscle elements to follow the curvature of the vertebrae. Therefore, half of the vertebrae had to be defined as rigid and the two models I and II were developed according to Table I. To simulate both active and passive material properties of the musculature, two parallel spring elements were used where one was assigned passive and the other active muscle properties. The passive properties of the muscle groups were governed by bilinear curves. The bilinear properties were taken from an approximation of the stress-strain curve of structural failure muscle tests of rabbits performed by Myers et al. (1995). This was done using the physiologic cross section area (PCSA) and the meridian length of the modeled muscles which were retrieved from a report by Van Ee et al. (2000) for all muscle groups except four where values were estimated from anatomical sketches by Kapandji (1974), Table II. The active part of the muscle force was modeled with Hill-elements by defining the optimal muscle length (L_{opt}) for each muscle, the peak force (F_{max}) generated by the muscle, and a curve defining the level of activation as a function of time. The optimal length was calculated from the average rest length (initial upright position of the model) of the spring elements representing each individual muscle group. This is a minor simplification as all muscles in the cervical spine have reported optimal length close to the rest length, van der Horst (2002). The peak force was calculated from the PCSA and a peak muscle stress of 50 N/cm^2. This value for the peak muscle stress was adopted from Winters and Stark (1988). Table II lists the values used to define the active properties for each group of muscles. At the time of activation (T_{act}) the activation force increases piecewise-linearly from zero to F_{max} at full activation 100 ms later according to Figure 2A. T_{act} is defined as the sum of the time from the start of the impact to the time when a sensory threshold is exceeded plus the neural reflex time. It is assumed that muscle activation is triggered

Table II The Physiologic Cross Section Area (PCSA) [Van Ee] and the active properties defined for each muscle

	No of springs	Parallel springs	Scale	PCSA (cm^2)	L_{opt} (mm)	σ_{max} (N/cm^2)	F_{max} (N)
SCOM	24	4	3	4.92	51	50	82
Longus Cervicis	19	1	4	1.37	60	50	17
RAMa*	8	1	4	1.68	85	50	21
RAMi*	4	1	1	0.92	30	50	46
Scalene	24	1	12	4.29	120	50	18
Suboccipital*	8	1	1	1.00	30	50	50
Semispinalis	40	4	8	8.58	27	50	54
Longissimus	62	4	10	2.47	35	50	12
Splenius	40	4	10	4.52	80	50	23
Levator scapulae	32	4	4	3.12	41	50	39
Trapezius	66	4	9	13.73	41	50	76
Interspinous*	5	1	1	1.00	14	50	50
Hyoid superior	3	1	1	1.02	30	50	51
Hyoid inferior	2	1	12	1.33	120	50	67

*Estimated values of PCSA from anatomy literature, Kapandji (1971).

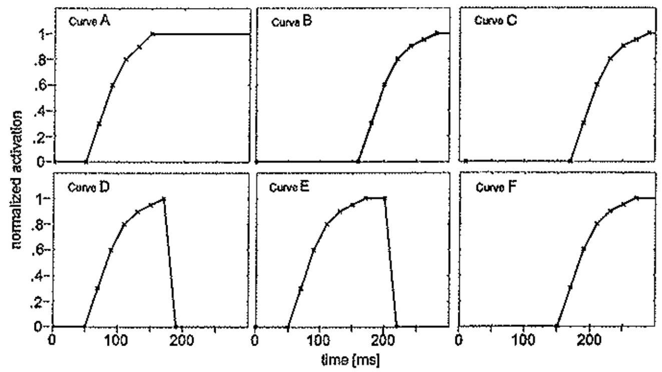

Figure 2 Curves used to define the active muscle properties as a function of time, during simulation of the frontal and lateral impacts.

by motion of the lower cervical spine, as suggested by Szabo and Welcher (1996), hence T_{act} is couple to the T1 acceleration. Muscle activation is described by neural excitation and active state dynamics, this has been simplified by describing the muscle force as increasing piecewise linearly with time after T_{act}. A full activation after 100 ms is assumed, which is based on a report by Winters and Stark (1985).

The complete FE models with active muscle properties were compared to sled tests performed on human volunteers at the Naval Biodynamics Laboratory by Ewing et al. (1976a, b). The subjects were seated in an upright position on a rigid seat and exposed to short duration acceleration pulses in two different directions, simulating frontal and side impacts. The subjects were restrained with shoulder, lap, and chest belts. For the frontal impact, the maximum acceleration was 15 g and the impact velocity was 16.7 m/s (60 km/h). The side impact had a maximum acceleration of 7 g and an impact velocity of 6.94 m/s (25 km/h). In these tests the three-dimensional motions of the head and the first thoracic vertebra (T1) were recorded using accelerometers and photographic targets. Five subjects were participating in nine tests for the frontal impacts while nine subjects participated in nine tests for the lateral impacts. All subjects were young and well trained men. These experiments were simulated with the KTH model by prescribing the experimental velocity-time data of T1 to the cube inferior to C7. No other constraints or boundary conditions were applied to the FE model. The resulting relative motion of the skull compared to T1 was measured and compared to the corridors from the volunteer experiments. Gravity was neglected in the numerical simulations to obtain a stable initial position of the head. Based on the onset of T1 accelerations the values for T_{act} were chosen to 50 ms for both impacts.

A small parameter study was performed to evaluate the influences of the generated muscle force, F_{max}, on the neck response by scaling the curves in Figure 2A to represent activation levels of 20, 40, 60, and 100 percent of the maximum muscle stress (50 N/cm^2). To evaluate the effect of the duration of muscle activation the curve in Figure 2 was modified to include decrease of activation, Figure 2D–F. Also, the interaction and varied response of muscle agonists and antagonist was simulated by assigning different activation curves to different muscle groups. In the frontal impact the main extensor muscles were activated prior to the flexors. In the side impact the ipsilateral muscles were activated prior to the contralateral muscles. For simplicity, all muscles were activated to the same activation stress. All the simulated muscle activation configurations are listed in Table III with activation curves defined by Figure 2. In all these simulations the passive properties of the musculature were unchanged.

Lastly, the FE models were used to study vertebral stresses and ligament strain for varied levels of muscle activation. The frontal and lateral impacts from the sled tests by Ewing were chosen as load cases and the model configurations used were "Comb2" and "Comb3" from Table III.

RESULTS

Frontal Impact

Figure 3 shows the response of the FE model depending on the muscle activation properties. The motion of the head compared to the thorax cube is plotted. It is clear that the FE model with only passive muscle properties has a weaker response than the volunteers. All the activation configurations have a better response compared to the experiments than the passive model. The models with peak muscle stress of 50 N/cm^2 all lie more or less within the corridors, whereas the 60% activation gives a slightly too flexible model. It is evident that a decrease of the activation after some time (All2) broadens the response curve and increases the time of the head motion. The configuration with best response is Comb2. Therefore, the peak muscle stress was varied for this configuration. Figure 4 illustrates how the relative motion between the head and the thorax is affected by scaling of the peak muscle force. Less than 60% activation gives a model that has a too weak response. An 80% or full activation (Comb2 80% and Comb2) shows good correlation for flexion and eliminates the bounce in anterior-posterior translation evident for the weaker muscle models. The model with full activation is slightly to stiff for superior-inferior translations, whereas the

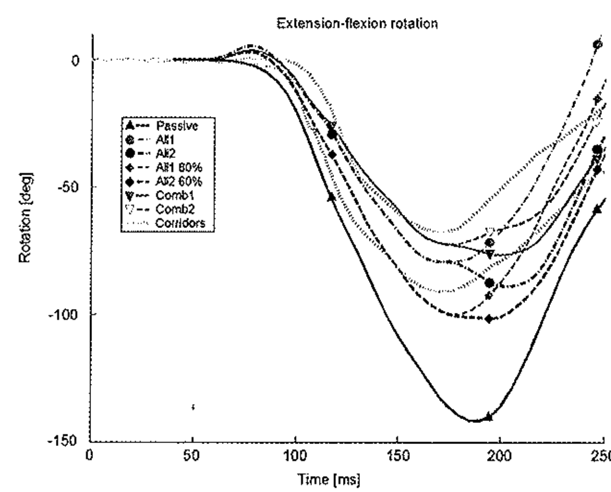

Figure 3 The relative flexion-extension rotation between the head and the thorax cube for the frontal impact. FE model responses for peak muscle stress of 50 N/cm^2 and varied activation curves compared with corridors from volunteer sled test by Ewing et al. (1976a, b). Model I.

Table III List of simulations. The activation levels of the different muscles have been scaled from 100%, which represents a peak muscle stress of 50 N/cm^2. The activation curves are defined in Figure 2.

Frontal impact Muscle groups	Passive act	Curve	All1 Act	All1 80% Act	Curve	All2 Act	All2 80% Act	Curve	Comb1 Act	Curve	Comb2 Act	Comb2 80% Act	Comb2 60% Act	Comb2 40% Act
SCOM	0%	A	100%	60%	D	100%	60%	B	100%	F	100%	80%	60%	40%
Longus Cervicis	0%	A	100%	60%	D	100%	60%	B	100%	F	100%	80%	60%	40%
R. A. Ma.	0%	A	100%	60%	D	100%	60%	B	100%	F	100%	80%	60%	40%
R. A. Mi	0%	A	100%	60%	D	100%	60%	B	100%	F	100%	80%	60%	40%
Scalene	0%	A	100%	60%	D	100%	60%	—	0%	—	0%	0%	0%	0%
Suboccipital	0%	A	100%	60%	D	100%	60%	D	100%	E	100%	80%	60%	40%
Semispinalis	0%	A	100%	60%	D	100%	60%	D	100%	E	100%	80%	60%	40%
Longissimus	0%	A	100%	60%	D	100%	60%	D	100%	E	100%	80%	60%	40%
Splenius	0%	A	100%	60%	D	100%	60%	D	100%	E	100%	80%	60%	40%
Levator scapulae	0%	A	100%	60%	D	100%	60%	D	100%	E	100%	80%	60%	40%
Trapezius	0%	A	100%	60%	D	100%	60%	D	100%	E	100%	80%	60%	40%
Interspinous	0%	A	100%	60%	D	100%	60%	D	100%	E	100%	80%	60%	40%
Hyoid superior	0%	A	100%	60%	D	100%	60%	B	100%	F	100%	80%	60%	40%

Side impact Muscle groups	Passive Act	Curve	Half 60% Act	Curve	All 60% Act	Curve	Combo3 Act	Combo3 60% Act	Combo3 40% Act
Ipsilateral	0%	E	60%	E	60%	E	100%	60%	40%

80 percent model is within the experimental corridors. Therefore, the Comb2 80% model has the best correlation. Figure 5 compares the neck kinematics for the passive model and the Comb2 80% model.

The maximum von Mises stress in the vertebral trabecular bone averaged 6 MPa for all simulations and vertebrae, except for C1 and C2. The reported compression failure stress of 10 MPa (Carter & Hayes, 1977) was exceeded in C2 for the passive model and in C1 for the cases with 60%, 80%, and 100% activation. For the vertebral cortical bone the maximum von Mises stress averaged 90 MPa with one exception. In the passive model C2 had a peak stress of 1200 MPa due to a concentrated nodal load. There was no apparent trend between the maximum von Mises stress and the level of activation.

The effect of muscle activation on the responses of the spinal ligaments is displayed in Table IV. The maximum displacements are normalized to tensile failure data from the literature, listed with references in Table IV. The lower cervical spine, and especially the interspinous ligaments and the ligamentum flavum, is critical with values above 1, which predicts failure. Muscle activation significantly decreases the risks for injuries of the spinal ligaments.

Lateral Impact

The relative motion between the head and the thorax due to a side impact is plotted in Figure 6. The FE model with only passive properties is much too weak in lateral bending compared to the response of the volunteers, while the active models correlate better. The best correlation was achieved by Comb3 60% and therefore, this configuration was used to vary the peak muscle stress. Figure 7 illustrates the relative head and thorax response to 40, 60, and 100% of the peak muscle stress (50 N/cm^2). Model Comb3 40% has a good correlation for the lateral bending and axial rotation, and is mostly within the corridors for extension. This model has a peak muscle stress of approximately 20 N/cm^2. The coupled motions do not have the same correlation. The volunteers had some coupled extension of the neck, where the passive model goes into flexion and the active models have too large extension rotations. Figure 8 compares the neck motion for the passive model and Comb3 40%.

The maximum von Mises stress levels in the vertebral cortical bone averaged 130, 152, and 157 MPa for the passive, the Comb3 40% and the Comb3 60% models respectively. The compression failure tolerance of 200 MPa for cortical bone reported by Carter and Hayes (1977) was only exceeded in C2 (220 MPa) and C5 (270 MPa) for the Comb 60% model. The maximum trabecular bone von Mises stresses averaged 5 MPa for all simulations and vertebrae, except for C1 and C2. The passive and Comb3 60% models displayed high stresses (30 and 20 MPa) in C1 due to nodal forces. The Comb 3 40% model had a maximum von Mises stress of 11 MPa at C2, which exceeds the failure value of 10 MPa reported by Carter and Hayes (1977).

The spinal ligaments in motion segments C2–C3 and C4–C5 are most strained by this side impact, Table IV. The passive model predicts failure for the capsular ligaments while activation decreases the tension of the ligaments below the used tissue level threshold. Overall, activation of the musculature decreases the risk for ligamentous injuries.

DISCUSSION

The purpose of this study was to improve and validate a detailed FE model of the cervical spine and musculature, the KTH model. The effect of muscle activations on spinal responses were evaluated for frontal and side impacts. Implementing both active and passive properties of the muscles gave a better correlation to the experimental volunteer data than the FE model with only passive muscle properties. The KTH model has several limitations.

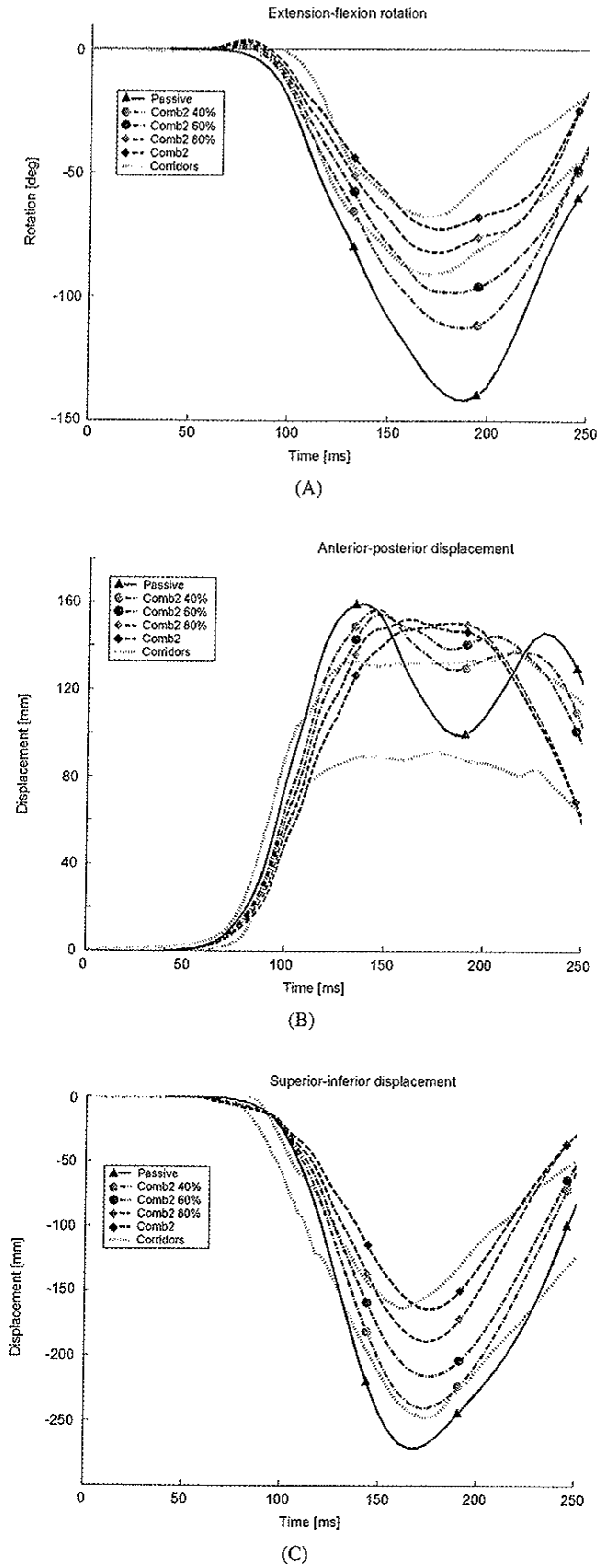

Figure 4 Varied peak muscle stress for Model I (Comb2), response due to a frontal impact with corridors from volunteer sled test by Ewing et al. (1976a, b). The relative motion between the head and the thorax cube for: (A) flexion-extension rotation, (B) anterior-posterior, and (C) superior-inferior displacements.

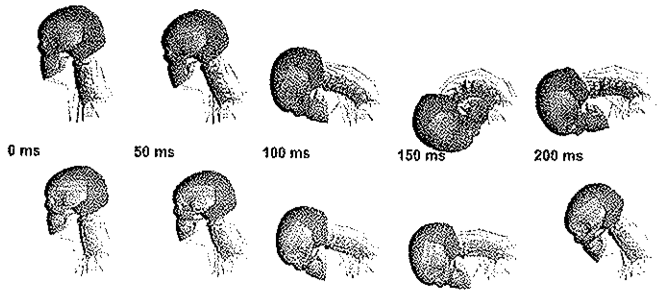

Figure 5 Neck motion during a frontal impact for an FE model with passive muscles (top); and active muscles according to Comb2 80% (bottom).

The muscles are simplified with spring elements and therefore the muscle force has a straight line of action. To account for the neck curvature the more superficial muscles were divided into four serial spring elements. The nodes connecting these elements were merged with a rigid vertebra. The benefit of this solution is curved lines of action for the large muscles and the major drawback is the limitation that some of the vertebrae have to be rigid. To study the vertebral stresses a solution with two models was picked, where every second vertebra was rigid so that the muscles could be merged. Some muscles nodes were merged with a neighboring vertebra instead of the closest vertebra which gave a slightly different response. Also, the muscles response influenced the motion of the vertebrae they were connected with to some extent. To ensure that both elastic-rigid models behaved appropriately and realistic they were compared with good correlation to two all-rigid models with and without muscle-vertebrae connections.

The frontal impact in this study was a volunteer experiment with an impact velocity of 60 km/h, while the side impact had a lateral velocity of 25 km/h. The KTH model correlated best to the volunteer data for the side impact when the peak muscle activation was 40% of the peak muscle stress, whereas a peak muscle activation of 80% gave the best response compared to

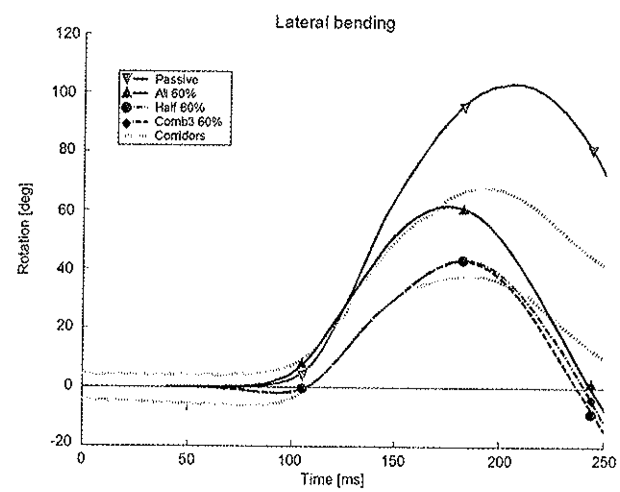

Figure 6 The relative lateral bending rotation between the head and the thorax cube for the lateral impact. FE model responses compared with corridors from volunteer sled test by Ewing et al. (1976a, b). 60% of the peak muscle stress (30 N/cm^2) for varied activation curves. Model II.

Table IV Ligament responses due to the frontal and side impacts. The maximum elongations are scaled by failure tolerances (D_f) reported in the literature and hence a value of 1 predicts failure.

	Frontal impact					Lateral impact			Used for failure analysis	
	Passive	Comb2 40%	Comb2 60%	Comb2 80%	Comb2	Passive	Comb3 40%	Comb3 60%	D_f (mm)	Reference
Upper cervical spine: C0-C2										
Alar	0.51	0.28	0.15	0.08	0.07	0.60	0.46	0.48	14	Dvorack et al. (1988), Yoganandan et al. (2001)
Apical	0.88	0.52	0.32	0.19	0.16	0.63	0.41	0.24	10	Yoganandan et al. (2001)
VC	0.54	0.41	0.30	0.22	0.21	0.73	0.45	0.23	25	Yoganandan et al. (2001)
AAOM	0.19	0.21	0.20	0.12	0.11	0.11	0.15	0.12	19	Yoganandan et al. (2001)
TM	0.75	0.37	0.17	0.06	0.01	0.61	0.32	0.12	12	Yoganandan et al. (2001)
PAOM	0.85	0.48	0.35	0.41	0.35	0.61	0.25	0.13	18	Yoganandan et al. (2001)
ALL C1–C2	0.59	0.34	0.22	0.22	0.21	0.45	0.32	0.18	10	Yoganandan et al. (2001)
LF C1–C2	0.84	0.22	0.08	0.00	0.00	0.42	0.01	0.00	9	Yoganandan et al. (2001)
CL C0–C1	0.49	0.29	0.22	0.32	0.36	0.79	0.45	0.34	10	Yoganandan et al. (2001)
CL C1–C2	0.53	0.35	0.32	0.52	0.38	0.95	0.59	0.63	9	Yoganandan et al. (2001)
C2–C3										
ALL C2–C3	0.09	0.06	0.15	0.21	0.18	0.32	0.25	0.32	10	Myklebust et al. (1988)
PLL C2–C3	0.42	0.33	0.28	0.13	0.12	0.70	0.39	0.19	7	Myklebust et al. (1988)
CL C2–C3	0.67	0.55	0.49	0.55	0.26	1.31	0.76	0.46	9	Myklebust et al. (1988)
LF C2–C3	0.83	0.66	0.61	0.38	0.25	0.99	0.54	0.37	8	Myklebust et al. (1988)
ISL C2–C3	1.85	1.59	1.54	0.91	0.76	1.28	0.40	0.00	7	Myklebust et al. (1988)
C3–C4										
ALL C3–C4	0.01	0.00	0.02	0.06	0.02	0.30	0.33	0.34	10	Myklebust et al. (1988)
PLL C3–C4	0.38	0.36	0.32	0.24	0.18	0.70	0.38	0.24	7	Myklebust et al. (1988)
CL C3–C4	0.60	0.58	0.52	0.33	0.29	1.19	0.84	0.89	9	Myklebust et al. (1988)
LF C3–C4	0.95	0.91	0.81	0.50	0.42	0.84	0.44	0.52	8	Myklebust et al. (1988)
ISL C3–C4	1.98	1.93	1.77	1.23	1.05	0.93	0.00	0.00	7	Myklebust et al. (1988)
C4–C5										
ALL C4–C5	0.02	0.01	0.00	0.02	0.04	0.33	0.33	0.25	10	Myklebust et al. (1988)
PLL C4–C5	0.45	0.45	0.44	0.58	0.58	0.68	0.40	0.19	7	Myklebust et al. (1988)
CL C4–C5	0.70	0.69	0.67	0.87	0.87	1.13	0.74	0.53	9	Myklebust et al. (1988)
LF C4–C5	1.06	1.06	1.02	1.36	1.37	0.85	0.54	0.34	8	Myklebust et al. (1988)
ISL C4–C5	2.05	2.01	2.00	2.48	2.49	0.91	0.04	0.06	7	Myklebust et al. (1988)
C5–C6										
ALL C5–C6	0.00	0.00	0.00	0.00	0.00	0.28	0.22	0.19	10	Myklebust et al. (1988)
PLL C5–C6	0.62	0.54	0.54	0.63	0.64	0.60	0.39	0.32	7	Myklebust et al. (1988)
CL C5–C6	0.90	0.85	0.83	0.99	0.98	0.97	0.63	0.54	9	Myklebust et al. (1988)
LF C5–C6	1.60	1.50	1.46	1.69	1.66	0.68	0.48	0.41	8	Myklebust et al. (1988)
ISL C5–C6	2.25	2.10	2.05	2.33	2.29	0.54	0.31	0.29	7	Myklebust et al. (1988)
C6–C7										
ALL C6–C7	0.01	0.00	0.00	0.00	0.00	0.19	0.14	0.16	10	Myklebust et al. (1988)
PLL C6–C7	0.81	0.67	0.68	0.72	0.57	0.45	0.31	0.26	7	Myklebust et al. (1988)
CL C6–C7	1.09	0.93	0.92	0.98	0.87	0.77	0.54	0.48	9	Myklebust et al. (1988)
LF C6–C7	2.16	1.84	1.84	1.91	1.76	0.53	0.36	0.31	8	Myklebust et al. (1988)
ISL C6–C7	3.12	2.70	2.69	2.79	2.54	0.33	0.46	0.45	7	Myklebust et al. (1988)

the frontal impact. Also, higher or lower activation forces gave a decrease in the correlation with the experiments. This was particularly evident for how the coupled rotations in lateral bending compared to experimental data. It seems that to obtain the best response of an FE model different peak muscle forces have to be chosen depending on the load case studied. Hence, it is important to pick activation parameters relevant to the degree and direction of impact for each numerical simulation performed. This is one of the challenges in numerical modeling of active musculature since experimental data on muscle activity and neck responses suitable for validation is scarce. Until this experimental data is available, it is suggested that the active muscle properties of numerical models are tuned to correlate with experimental data relevant to the load cases studied.

Muscle activation reached the peak muscle force after 100 ms. This was based on other studies on the delay in neural reflexes and the time from impact until a neural response is triggered, Winters and Stark (1985). It was assumed that the onset of acceleration for T1 triggers the neural responses and time of muscle activation, as suggested by Szabo and Welcher (1996). Their results indicated that muscle recruitment was centrally generated and consistently found that the onset of lumbar spine acceleration correlated with neck muscle activation 90–120 ms later, for rear end impacts. For a frontal or lateral impact the lower spine and chest will experience the impact through interaction with seat belts before the cervical spine and head acceleration starts. In the rear end impact the interaction with the seat back causes the same kind of response. Therefore, it was assumed to

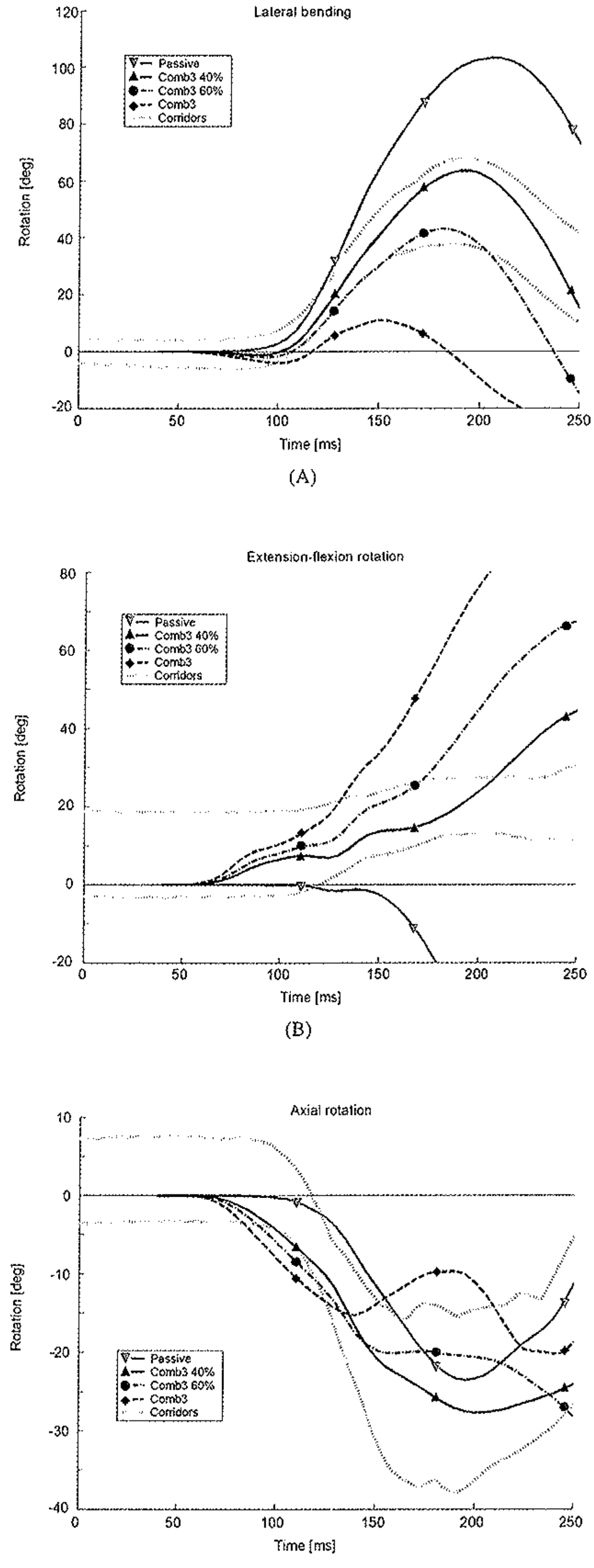

Figure 7 Side impact responses due to varied peak muscle stress for Model II (Comb3) with corridors from volunteer sled test by Ewing et al. (1976a, b). The relative motion between the head and the thorax cube for: (A) lateral bending, (B) flexion-extension, and (C) axial rotation.

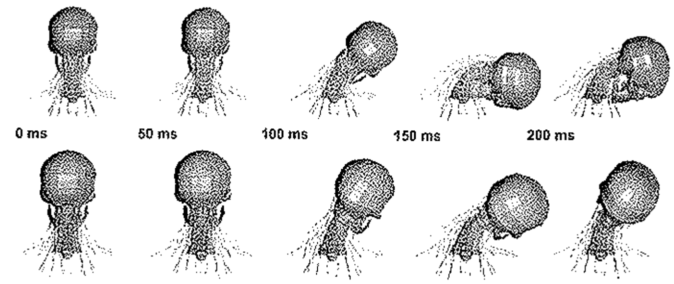

Figure 8 Neck motion during a side impact simulation for an FE model with passive muscles (top); and active muscles according to Comb3 40% (bottom).

be realistic to use the onset of T1 acceleration as a trigger for neck muscle activation in these simulations of frontal and lateral impacts. An electromyography (EMG) study with surface electrodes conducted by Lu and Bishop (1996) of short dynamic lateral bending showed that the peak EMG was between 75 and 165 ms later than the peak applied force. This correlates to the reaction and activation time of 150 ms used in the lateral simulations. It was considered inappropriate to maintain full activation after the peak motion had occurred, that is during the rebound phase. As expected, the configurations were full activation was maintained once it had been reached had a faster response and a larger opposite motion. To evaluate the importance of implementing the decrease of activation in response to the directional change of head motion, the activation curve was dropped from full activation to zero in 20 ms. In the dynamic lateral bending study by Lu and Bishop (1996), the decrease of the EMG signal was slightly slower than the increase. Therefore, our activation decrease is a too fast scenario but it gives an idea of the importance of implementing deactivation. It was evident that the FE model had a better correlation to the volunteer corridors when activation was decreased.

Another aspect of activation is muscle synergies. In the experiments by Lu and Bishop (1996) the contra-and ipsi-lateral muscles demonstrated different EMG profiles. The EMG signals were in some cases 20 percent of the ipsilateral signals. The significance of this synergism was evaluated by activating only the ipsilateral muscles in the beginning of the side impact and the contralateral muscles in the rebound phase of the impact. This significantly improved the correlation of the coupled rotations in the side impact. Also, Kumar et al. (2003) performed a study of frontal impacts that measured the reaction times of the muscles with both surface and wire electrodes. The results of this study showed that the antagonistic muscles, in this case the flexors reacted much later than the extensors. Therefore, simulations were performed where the extensors were activated at 50 ms and the flexors during the rebound phase. The response was improved, though not as significantly as for the side impact. It can be concluded that inclusion of muscle synergism in an FE model with active muscles improves the correlation. It would be interesting to control activation of muscles in an FE model using EMG curves. Dynamic studies where both EMG and vertebral rotations and head motion is monitored would be a valuable source of information for validation of numerical model.

The maximum von Mises stress in the cortical and trabecular bone was studied for all simulations. Carter and Hayes (1977) have reported compression failure stresses for the cortical of approximately 200 MPa and for the trabecular bone of 10 MPa at a strain rate of about 1. The average von Mises stresses did not exceed these values for neither the trabecular nor the cortical bone in any of the simulations. In the frontal impact, activation of the musculature did not affect the average vertebral stresses. For the side impact a slight increase of the von Mises stress in the cortical bone could be seen for increasing activation, though there was not a significant difference. In a few simulations high nodal forces were induced by the muscle elements in the shell and solid elements of the vertebrae at the location of muscle insertion. Therefore, it is suggested to model the musculature with more geometrical detail to accurately transfer forces between the musculature and the vertebrae.

Soft tissue injuries have become increasingly important since the Whiplash discussion started. High cost to society and insurance costs as well as suffering for the individuals have put focus on the soft tissue injuries. Failure or sub-failure of ligaments is a candidate explanation for some of these injuries. It is possible to evaluate the effect of muscle activation on the soft tissue response. The KTH model has a detailed representation of the spinal ligaments and the strain data was evaluated and compared to experimental failure deformations to predict soft tissue injury. This study showed that the posterior ligaments in the lower cervical spine took much of the loading in the frontal impact, while the posterior ligaments and the capsular ligament in the central cervical spine took most of the loading for the side impact. Failure was only predicted for the side impact when the muscles were not activated. Thus, muscle activation reduced the risk of injury to the capsular ligaments and the interspinous ligaments. The stretches of the other ligaments were also reduced. For the frontal impact, the KTH model predicted injury to the interspinous ligaments on spinal levels C2 to C4 for no and for low activation levels while full activation reduced the risk significantly. In the lower cervical spine injury was predicted for the interspinous ligament and the ligamentum flavum with and without activation. The volunteer experiments by Ewing did not report any neck complaints and there are some possible explanations to why the KTH model did. The FE model was constrained for all degrees of freedom at the C7 vertebrae and the thorax cube. This boundary condition is a simplification of the belted volunteers, who's T1 were allowed to rotate and thereby transmit some motion below the seventh vertebra. Thus, the FE model is loaded more severely than the volunteers and this is presumably worst for the lower and posterior cervical spine. Another limitation is the tissue level injury threshold used for normalizing the deformation, which is some cases are based on less than five cervical spine specimens. The individual variation is large and it could be relevant to use a higher value for the tissue level criteria for the ligamentum flavum and the interspinous ligament.

It is interesting to note that muscle activation for the frontal impact mainly reduces the loading of the upper cervical spine ligaments. In the lateral loading all spinal levels were equally protected by muscle activation. Van Ee et al. (2000) and Chancey et al. (2003) found that activation of the neck muscles mainly shields the lower cervical spine for a tension loading case. These contrasting results suggest that the spinal musculature has different protective properties depending on the external loading that the neck is subjected to.

CONCLUSION

An anatomically detailed FE model with active muscles that follow the spinal curvature has been developed and validated against frontal and side impacts with good correlation. Also, muscle synergism was implemented in the model with good results. The current model was used for injury prediction of soft tissues using tissue specific failure criteria during dynamic loading. Muscle activation was found to decrease the risk of injury to the spinal ligaments. Activation protects the upper cervical spine in frontal impacts where injury was predicted with a passive muscle model. In lateral impacts, muscle activation decreased ligaments strain at all spinal levels. It can be concluded that muscle activation decreases the risk for ligamentous injury, and that the spinal levels that are protected varies with the external loading that the neck is subjected to.

ACKNOWLEDGMENT

The original version of this paper was presented at the NATO Research and Technology Organization (RTO) Symposium, reference AVT-097—Joint AVT/HFM Specialists' Meeting on "Equipment for Personal Protection." The paper will be published by the RTO as part of Meeting Proceedings MP-108 entitled "Equipment for Personal Protection." Along with all scientific publications produced by the RTO, this report will be made available on the RTO website, www.rta.nato.int.

REFERENCES

Brolin K. (2002) Cervical Spinal Injuries—Numerical Analyses and Statistical Survey. *Doctoral Thesis*, Report 2002-29, The Royal Institute of Technology, Department of Aeronautics, Stockholm, Sweden.

Brolin K. (2003) Neck Injuries among the Elderly, a National Survey in Sweden from 1987 to 1999. *Injury Control and Safety Promotion*, Vol. 10, No. 2, pp. 155–162.

Brolin K, Halldin P. (2003) Development of a finite element model of the upper cervical spine and a parameter study of ligament characteristics, *SPINE* (to be published).

Brolin K, von Holst H. (2002) Cervical Injury in Sweden, a National Survey of Patient Data from 1987 to 1999, *Injury Control and Safety Promotion*, Vol. 9, No. 1, pp. 40–52.

Carter D, Hayes W. (1977) The compressive behavior of bone as a two phase porous structure, *J. Bone and Joint Surgery*, Vol. 59A, No. 7, pp. 954–962.

de Jager M, Sauren A, Thunissen J, Wismans J. (1994) A three-dimensional head-neck model: validation for frontal and lateral impacts. Proceedings of the 38th *Stapp Car Crash Conference*, 942211.

de Jager M, Sauren A, Thunnissen J, Wismans J. (1996) A global and a detailed mathematical model for head-neck dynamics. Proceedings of the 40th *Stapp Car Crash Conference*, 962430.

DeVito C, Lambert D, Sattin R, Bacchelli S, Ros A, Rodrigues J. (1988) Fall injuries among the elderly, community based surveillance, *J Am Geriatrics Society*, Vol. 36, pp. 1029–1035.

Dvorack J, Schneider E, Saldinger P, Rahn B. (1988), Biomechanics of the craniocervical region: the alar and transverse ligaments, *J Orthopaedic Research*, No. 6, pp. 452–461.

Ewing CL, Thomas DJ, Lustick L, Muzzy III WH, Williams G, Majewski PL. (1976a) The Effect of Duration, Rate of Onset and Peak Sled Acceleration on the Dynamic Response of the Human Head and Neck. Proceedings of the *20th Stapp Car Crash Conference*.

Ewing CL, Thomas DJ, Lustick L, Muzzy III WH, Williams GC, Majewski P. (1976b) Effect of Initial Position on the Human Head and Neck Response to +Y Impact Acceleration. Proceedings of the 20th *Stapp Car Crash Conference*.

Goel VK, King Liu Y, Clark CR. (1986) Quantitative Geometry of the Muscular Origins and Insertions of the Human Head and Neck, Mechanisms of Head and Spine Trauma, Chapter 13, pp. 397–415, *Aloray Publisher*.

Goel V, Winterbottom J, Schulte K, Chang H, Gilbertson L, Pudgil A, Gwon J. (1990) Ligamentous Laxity Across C0-C1-C2 Complex Axial Torque-Rotation Characteristics Until Failure. *SPINE*, Vol. 15, No. 10, pp. 990–996.

Gray H. (2002) Gray's Anatomy of the Human Body, http://www.Bartleby.com/107/, date: 2002-09-23.

Halldin P. (1998) Injury prevention and numerical modeling of the human head and neck, *Licentiate Thesis*, Report 98-7, Royal Institute of Technology, Department of Aeronautics, Stockholm, Sweden.

Halldin P. (2001) Prevention and prediction of head and neck injury in traffic accidents—using experimental and numerical methods. *Doctoral Thesis*. Report 2001-1, Royal Institute of Technology, Department of Aeronautics, Stockholm, Sweden.

Halldin P, Jakobsson L, Brolin K, Palmertz C, Kleiven S, von Holst H. (2000) Investigation of Conditions that Affect Neck Compression-Flexion Injuries Using Numerical Techniques. *The 44th STAPP Car Crash Journal*, 2000-01-SC10.

Hallquist JO. (1998) LS-DYNA Theoretical Manual, *Livermoore Software Technology Corporation*.

Hoskin A. (2000) Tends in unintentional-injury deaths during the 20th century. *Statistical Bulletin*, Metropolitan insurance companies, Vol. 81, pp. 18–26.

Jost R, Nurick GN. (2000) Development of a finite element model fo the human neck subjected to high g-level deceleration, *Int J Crashworthiness*, Vol. 5, pp. 259–267.

Kapandji IA. (1974) The Physiology of the Joints, Volume 3 The trunk and vertebral column, Second edition, *Churchill Livingstone*, Edinburgh, London and New York.

Kleiven S. (2002) Finite Element Modeling of the Human Head, *Doctoral, Thesis* Report 2002-9, Royal Institute of Technology, Department of Aeronautics, Stockholm, Sweden.

Leijonhufvud I. (2001) Development of an inner car roof design and implementation of muscles in a numerical model of the human neck. *Master Thesis*. Report 2001-43, Royal Institute of Technology, Department of Aeronautics, Stockholm, Sweden.

Liu Y, Krieger K, Njus G, Ueno K, Connors M, Wanako K, Thies D. (1980) Cervical Spine Stiffness and Geometry of the Young Human Male, AFAMRL-TR-80-138. *Air Force Aerospace Medical Research Lab.* USA.

Lomoschitz F, Blackmore C, Mirza S, Mann F. (2002) Cervical spine injuries in patients 65 years old and older: epidemiologic analysis regarding the effects of age and injury mechanism on distribution, type and stability of injuries. *AJR Am J Roentgenol*, Vol. 178, No. 3, pp. 42–47.

Lu W, Bishop P. (1996) Electromyographic Activity of the Cervical Musculature during Dynamic Lateral Bending. *SPINE*, Vol. 21, pp. 21, pp. 2442–2449.

Myers BS, Van Ee CA, Camacho DLA, Woolley CT, Best TM. (1995) On the Structural and Material Properties of Mammalian Skeletal Muscle and Its Relevance to Human Cervical Impact Dynamics, Proceedings of the 39th *Stapp Car Crash Conference*.

Myklebust JB, Pintar F, Yoganandan N, Cusick JF, Maiman D, Myers TJ, Sances A. (1988) Tensile strength of spinal ligaments, *SPINE*, Vol. 13, No. 5, pp. 526–531.

Nightingale RW, et al. (1996) Dynamic responses of the head and cervical spine to axial impact loading. *Journal of Biomechanics*, Vol. 29, No. 3, pp. 307–318.

Nightingale RW, et al. (1997) The dynamic responses of the cervical spine: buckling, end conditions and tolerances in compression impacts. *Proceedings for the 41st Stapp Car Crash Conference*, SAE 973344.

Panjabi MM, Dvorak J, Crisco III J, Oda T, Hilibrand A, Grob D. (1991a) Flexion, Extension, and Lateral Bending of the Upper Cervical Spine in Response to Alar Ligament Transections, *J Spinal Disorders*, Vol. 4, No. 2, pp. 157–167.

Panjabi MM, Dvorak J, Crisco III JJ, Oda T, Wang P, Grob D. (1991b) Effects of Alar Ligament Transection on Upper Cervical Spine Rotation, *J Orthopaedic Research*, Vol. 9, no. 4, pp. 584–593.

Szabo T, Welcher J. (1996) Human Subject Kinematics and Electromyographic Activity during Low Speed Rear Impacts. Proceedings for the 40th *Stapp Car Crash Conference*, SAE 962432, pp. 295–315.

Van der Horst. (2002), Human head neck response in frontal, lateral and rear end impact loading: Modelling and validation, Doctoral Thesis, Eindhoven Technische Universitet. ISBN 90-386-2843-9.

Van Ee CA, Nightingale RW, Camacho DLA, Chancey VC, Knaub KE, Sun EA, Myers BS. (2000) Tensile Properties of the Human Muscular and Ligamentous Cervical Spine. Proceedings of the 44th *Stapp Car Crash Conference*, 2000-01-SC07.

Winters J, Stark L. (1985) Analysis of fundamental human movement patterns through the use of in-depth antagonistic muscle model. *IEEE Transactions on Biomedical Engineering*, BME-32, pp. 826–839.

Winters J, Stark L. (1988) Estimated mechanical properties of synergistic muscles involved in movements of a variety of human joints, *J Biomechanics*, Vol. 21, No. 12, pp. 1027–1041.

Yang KH, Zhu F, Luan F, Zhao L, Begeman PC. (1998), Development of a finit element model of the human neck. Proceedings of the 42nd *Stapp Car Crash Conference*, 983157.

Yoganandan N, Kumaresan S, Pintar FA (2001) Biomechanics of the cervical spine. Part 2: Cervical spine soft tissue responses and biomechanical modeling, *Clinical Biomechanics*, Vol. 16, pp. 1–27.